Optically detected magnetic resonance study of SiC:Ti

K. M. Lee,* Le Si Dang,† and G. D. Watkins
Sherman Fairchild Laboratories and Department of Physics, Lehigh University, Bethlehem, Pennsylvania 18015

W. J. Choyke
Westinghouse Research and Development Center, Pittsburgh, Pennsylvania 15235
(Received 18 March 1985)

We describe optically detected magnetic resonance (ODMR) experiments carried out on the green luminescence band in $4H$, $6H$, and $15R$ polytypes of SiC:Ti. It is found that the luminescence is due to radiative transitions from excited spin triplet ($S=1$) to ground singlet ($S=0$) states. Unusually large isotope shifts in the zero-field splittings demonstrate that the light-emitting centers involve a single Ti and six equivalent neighboring silicon atoms. Spectral dependence studies of the ODMR signals allow us to discuss the microscopic nature of the inequivalent lattice sites for the Ti atom as well as to correctly assign the zero-phonon line and the accompanying characteristic phonons associated with each Ti site. We interpret our results in terms of the model proposed by Patrick and Choyke of Ti substituting on the silicon sublattice, the excitonic triplet state being formed from an electron tightly bound in a normally unoccupied d_e orbital of the Ti atom plus a Coulombically bound hole. The ODMR spectra are extremely sensitive to subtle (second- and third-nearest-neighbor) differences between the inequivalent lattice sites. This, plus a sizable Franck-Condon shift observed in the luminescence and the unusual isotope effects, are interpreted as possible evidence for vibronic properties of the bound hole, implying intermediate to strong localization for it also.

I. INTRODUCTION

Silicon carbide (SiC), a model group-IV-IV compound semiconductor, is an interesting material intermediate between silicon and diamond. Because of its high luminescence efficiency, SiC has been considered as a building block for optoelectronic devices such as light-emitting diodes, etc.[1] The crystal structure of SiC is complicated by the many possible stacking sequences of its Si-C layers, the so-called "polytypism." The crystallographic features of different polytypes can be characterized by the number of molecular layers in the repeating super cell as well as the overall crystallographic morphological structure. For example, the polytype $6H$ (or $4H$) means that the stacking sequence repeats every six (or four) layers and the morphological crystal structure is hexagonal (H). For the $15R$ polytype, the sequence repeats every 15 layers, producing a rhombohedral (R) crystal structure. There are two important consequences of the polytypism: a shift in the energy-band gap and differing numbers of inequivalent lattice sites. The existence of inequivalent sites is interesting because, by studying the site dependence of a defect, one can probe the effect on the electronic and vibronic properties of the defect of subtle environmental changes.

Since the discovery[2] of efficient green luminescence in $6H$ SiC at low temperature, the origin of the emission has been the subject of numerous investigations. Three sharp zero-phonon lines (hereafter noted as ZPL's), A_0, B_0, and C_0, were originally assigned as being due to bound-exciton decay at ionized nitrogen donors,[2] but this assignment was revised by Dean and Hartman,[3] who did magneto-optical studies on the sharp ZPL's. They observed spin-triplet-like Zeeman splittings with large zero-field splittings, from which they interpreted the origin of the ZPL's as bound-exciton decay at neutral isoelectronic centers.

The identity of the isoelectronic center was finally attributed to a Ti impurity by Choyke and Patrick after assigning the origin of fine structure seen in high-resolution spectra of the ZPL's as shifts due to the naturally abundant isotopes of Ti.[4] This was confirmed by Kemenade and Hagen, who performed selective Ti-isotope-doping experiments.[5]

Similar ZPL isotopic shifts were observed in polytypes other than $6H$ by Patrick and Choyke.[6] They correlated the number of ZPL's with the number of inequivalent lattice sites in a particular polytype (the site dependence). Another interesting fact they observed is that the ZPL energies are approximately constant, independent of the wide range of energy-band gaps for the various polytypes. Furthermore, for some polytypes ($3C$ and $21R$) which have energy-band gaps less than the energies of the ZPL's, no luminescence related to Ti was observed. They suggested that the energy-level position of the Ti-associated defect is independent of the conduction-band but locked to the valence-band edge. From this, they proposed a ligand theory model assuming the defect is an isoelectronic substitutional impurity on the Si sublattice.[6]

In this paper we report on optical detection of magnetic resonance (ODMR) experiments carried out on the green photoluminescence band in $4H$, $6H$, and $15R$ polytypes of SiC. The results show that the emitting states are indeed Ti-related spin-triplet states with axial symmetry along the crystallographic c axis. Particularly interesting is the observation of an unusually large isotopic mass effect on the fine-structure (D) term of the spin triplets. From a

detailed analysis of this isotopic effect, it is firmly established that the impurity center involves only one Ti atom, strongly interacting with a complex of six equivalent Si atoms. The role of the inequivalent lattice sites is also studied through a spectral dependence study of the ODMR signals which allows a correlation between the spin-triplet states and the ZPL's. Another interesting result of this study is the identification of the characteristic phonons associated with Ti on each inequivalent site. A short account of the ODMR results in the $6H$ polytype has been reported previously in Ref. 7.

II. EXPERIMENTAL RESULTS

A. Samples

Hexagonal SiC samples have a typical platelet shape. The flat faces of the platelet are (0001) growth planes, and the cleavage planes are both $(1\bar{1}00)$ and $(11\bar{2}0)$ planes. The samples used in this work were not intentionally doped. They were n type because of the natural nitrogen-donor background contaminant. Their polytype structure was determined by x-ray diffraction and confirmed by examining the photoluminescence spectrum. Figure 1, reproduced from Ref. 6, shows the energy positions of the ZPL's in $4H$, $6H$, and $15R$ SiC. The excitonic band gap E_{GX} and the number of inequivalent lattice sites are also shown. The labeling of the inequivalent sites follows the usual convention[1] and will be described in detail later in Sec. III C. The labeling of the ZPL's has been modified from that used in Ref. 6 according to the results obtained here by ODMR studies which will be discussed in Sec. III C.

B. Experimental techniques

ODMR experiments were carried out at 35 GHz in a TE_{011} cavity made up of concentric rings,[8,9] allowing a large aperture for the optical beams. Magnetic fields up to 3 T were produced by a superconducting magnet (modified SM-4, Oxford Instruments). The sample and resonant cavity were immersed in pumped liquid helium ($T \lesssim 2$ K).

The luminescence was excited with the uv lines of either a Kr- or Ar-ion laser, and detected by an RCA 4840 photomultiplier or an EG&G uv 250 silicon photodiode. Changes in the luminescence intensity due either to chopping of the microwave power ($\lesssim 50$ mW from a Gunn oscillator, CME 720) or magnetic field modulation ($\lesssim 1$ mT peak to peak (pp) at 1.25 kHz) were synchronously detected by a lock-in amplifier (Princeton Applied Research model 124). All measurements were made with the magnetic field rotating in a $(11\bar{2}0)$ plane.

A $\frac{1}{4}$-m grating monochromator (Jarrel-Ash Mark X) was used for spectral dependence studies. A stress modulator (Hinds International) was used for circular dichroism (CD) studies.

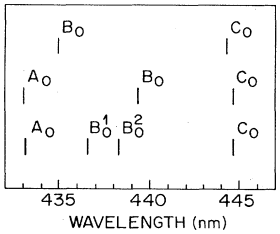

POLYTYPE	INEQUIVALENT SITES	E_{GX} (eV)
4H	h, k	3.265
6H	h, k_1, k_2	3.023
15R	h_1, h_2, k_1, k_2, k_3	2.986

FIG. 1. Energy positions of the ZPL's in various polytypes of SiC:Ti reproduced from Ref. 6. Shown also are the inequivalent lattice sites in the polytype structures. h and k represent hexagonal- and cubic-like inequivalent lattice sites, respectively.

C. ODMR study

The ODMR signals from the $4H$ and $15R$ polytype samples were found to be very similar to those observed in the $6H$ polytype samples. Therefore only the results obtained from $6H$ samples will be discussed in detail in the following.

Emission and excitation spectra of the luminescence in $6H$ SiC:Ti are shown in Figs. 2(a) and 2(b), respectively. The emission spectrum, obtained by exciting the sample with uv laser light, shows the resolved three ZPL's, A_0, B_0, and C_0, as well as their phonon replicas which merge to a broadband peaking at ~ 500 nm.

The excitation spectrum shown in Fig. 2(b), obtained by monitoring the low-energy portion of the luminescence band ($\lambda \gtrsim 500$ nm), is strongly suggestive that band-to-band transitions provide the most efficient excitation for the luminescence. The other figures in Fig. 2 will be discussed in later sections.

Figure 3 shows a typical ODMR spectrum of $6H$ SiC:Ti obtained by magnetic field modulation at $\theta = 0°$, where θ is the angle between the magnetic field and the hexagonal c axis of the crystal. The total emission from the sample was detected along the direction of the magnetic field. The magnetic field modulation was 0.5 mT (pp) at 1.25 kHz.

The lines in Fig. 3 can be divided into three groups: six microwave transitions (Ti_2^A, $Ti_{\pm 1}^A$, Ti_2^C, and $Ti_{\pm 1}^C$), two level-crossing signals (Ti_L^A and Ti_L^C; Ti_L^A is not apparent in the figure, but can be observed at higher modulation frequencies), and three cross-relaxation lines[10] (three sharp lines at $B < 0.2$ T). It will be shown later that the Ti^A and

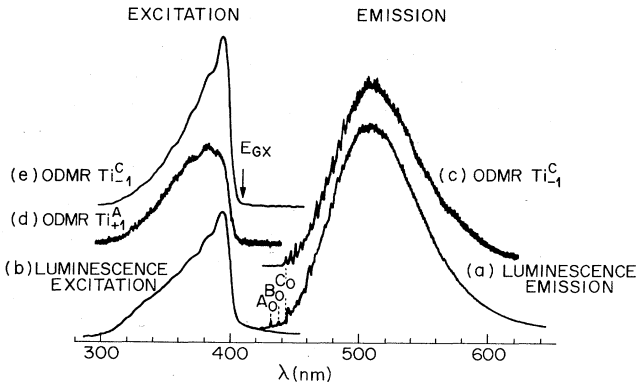

FIG. 2. Excitation and emission spectral dependences in $6H$ SiC:Ti.

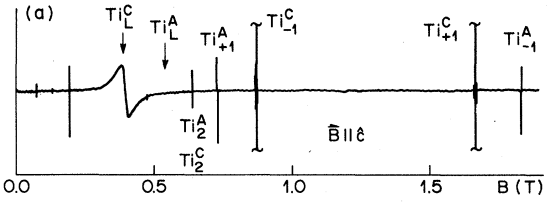

FIG. 3. Typical ODMR spectrum in 6H SiC:Ti obtained with magnetic field modulation at $\theta=0°$. The subscript 2 represents the $\Delta M=2$ resonance. Subscript $+1$ (-1) indicates the $\Delta M=1$ microwave transition involving the $|1,+1\rangle$ ($|1,-1\rangle$) state. L represents a level crossing.

Ti^C lines are correlated with the ZPL's, A_0 and C_0, respectively. The level-crossing and the cross-relaxation signals remain unchanged even when the microwaves are turned off. The broad level-crossing line disappears quickly when the c axis of the sample is rotated away from the magnetic field direction, providing a convenient way to orient the sample with respect to the magnetic field within an accuracy of $\pm 0.2°$.[10]

The central magnetic field positions of the six ODMR lines versus crystal orientation (θ) are shown in Fig. 4. The magnetic field was rotated in a $(11\bar{2}0)$ plane. The six curves in the figure can immediately be grouped into two sets, one shown with solid circles (Ti^A) and the other with open ones (Ti^C). The two higher-field lines of each set cross each other at $\theta=54.7°$, indicating that the splitting for each originates from a fine-structure interaction, with $S=1$. Their intensities reach a maximum at $\theta=0°$ and quickly decrease when θ is increased. They become zero at $\theta\sim 54.7°$. The signs of the $Ti^A_{\pm 1}$ lines reverse after the crossing while the Ti^C lines do not. The low-field lines (Ti^A_2 and Ti^C_2), on the other hand, have little anisotropy upon angular variation and their intensities become minimum and maximum at $\theta=0°$ and 45°, respectively.

Analysis of the angular dependence reveals two distinct spin-triplet ($S=1$) centers with the spin Hamiltonian

$$H=\mu_B \mathbf{B}\cdot\tilde{g}\cdot\mathbf{S}+D\left[S_z^2-\frac{S(S+1)}{3}\right]+\mathbf{S}\cdot\tilde{A}\cdot\mathbf{I}\,, \qquad (1)$$

where z denotes the c axis of the crystal, which also is the principal axis of the centers. The observed spin Hamiltonian parameters are also shown in Fig. 4. The solid curves in the figure are the theoretical fits obtained with Eq. (1) and the parameters. The last term in Eq. (1) represents the hyperfine (hf) interaction, which will be discussed in Sec. II C 2.

1. *Sign of D*

Several different experiments were performed to determine the signs of D for the spin triplets. Figure 5(a) shows the unpolarized total luminescence intensity monitored along the direction of the magnetic field, as a function of the magnetic field. The strong increase ($\sim 5\%$) in the total luminescence at $B\sim 0.4$ T (level crossing Ti^C_L) indicates that one of the Zeeman levels in Ti^C is a *bottleneck*. In other words, the accumulated population in

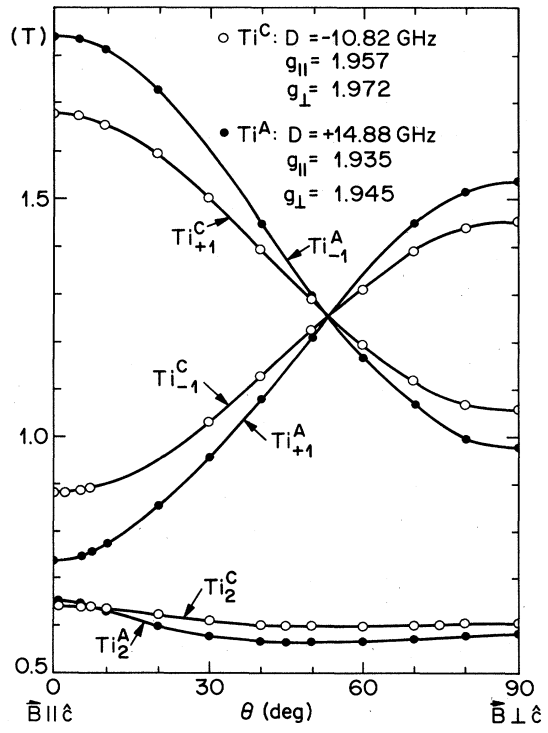

FIG. 4. Angular-dependent central magnetic field positions for the six ODMR lines as a function of θ. The magnetic field **B** is in a $(11\bar{2}0)$ plane.

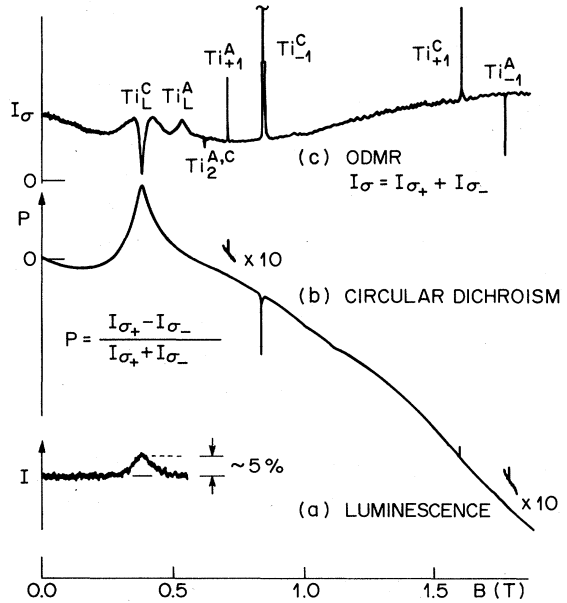

FIG. 5. Various signals plotted as a function of B at $\theta=0°$: (a) total luminescence, (b) circular dichroism in the total emission, and (c) ODMR signal obtained with microwave amplitude modulation.

the bottleneck state as a result of continuous optical pumping can be transferred to the radiative state by the level crossing, resulting in an increase in the emission intensity. The identity of the crossing levels can be determined by additional information, the light polarization of the emission.

Since the light polarization of emitted photons by optical dipole transitions is determined by the ΔM values, the strong increase in the σ_+ polarization at $B \sim 0.4$ T in Fig. 5(b) obtained by using a stress modulator demonstrates that the bottleneck and the radiative states undergoing the level crossing must be $|1,0\rangle$ and $|1,+1\rangle$, respectively. [The vertical axis of Fig. 5(b) represents $P = I_{\sigma_+} - I_{\sigma_-}$, where $I_{\sigma_\pm}$ are, respectively, the intensities of the $\sigma_\pm$ polarized light.] D of Ti^C therefore, is *negative* (see Fig. 6). This is also consistent with the signs of the ODMR signals, $Ti^C_\pm$, and the microwave-induced circular polarization as shown in Fig. 5(b). At both resonances ($Ti^C_{\pm 1}$), the population of the bottlenecked $|1,0\rangle$ state is the highest between the three states, and the microwave transitions equalize the populations, so that the net directions of the microwave transitions must be $|1,0\rangle \rightarrow |1,\pm 1\rangle$ which increase $I_{\sigma_\pm}$, respectively. This explains why both ODMR signals, $Ti^C_{\pm 1}$, in Fig. 5(c), are positive as well as why their microwave-induced polarizations are as shown in Fig. 5(b). [Luminescence propagating along $\mathbf{B} \| \hat{c}$ was detected to obtain the ODMR spectra. The ODMR, therefore, defects changes in the σ-component (both σ_+ and σ_-) light caused by microwave chopping or magnetic field modulation because only $\sigma_\pm$ components of the luminescence can propagate along $\mathbf{B}$. Actually, some depolarization occurs due to internal reflections, etc.]

On the other hand, the situation for Ti^A is different. First of all, the level-crossing signal, Ti^A_L, is not visible in the circular dichroism, Fig. 5(b). The sign of D, therefore, cannot be determined by polarization of the level-crossing signal. However, the ODMR signals and the microwave-induced polarization provide sufficient information to determine it.

Consider the ODMR signals Ti^A_{+1} and Ti^A_{-1} in Fig. 5(c). Their signs are opposite, which is consistent with the relevant directions of microwave transitions being $|1,0\rangle \rightarrow |1,+1\rangle$ (increase in I_{σ_+}) for Ti^A_{+1} and $|1,-1\rangle \rightarrow |1,0\rangle$ (decrease in I_{σ_-} for Ti^A_{-1}. This also is consistent with the sign of the microwave-induced polarizations [Fig. 5(b)] if the sign of D for Ti^A is positive and the spin-triplet Ti^A is thermalized (the lower-lying levels have more occupation than higher-lying ones).

Figures 6(a) and (b) show energy-level diagrams as a function of magnetic field, along with the directions of the microwave-induced transitions and their predicted results for Ti^C and Ti^A, respectively. The D values for both triplets confirm the magneto-optical measurements made by Dean and Hartman.[3] The bottleneck feature of Ti^C is consistent with Dean and Hartman's result in which they observed only the two $\Delta M = \pm 1$ optical transitions. For Ti^A, they observed all three lines ($\Delta M = 0, \pm 1$).[3]

The ODMR and level-crossing signals of Ti^C were optimized at a modulation frequency of ~ 1.25 kHz, while those of Ti^A continued to improve as the modulation frequency was increased up to the highest possible, ~ 10 kHz. Since the radiative lifetime of the ZPL's C_0 and A_0 is about the same ~ 100 μs,[11] this shows that the spin-lattice relaxation time is much longer for Ti^C than for Ti^A. This is fully consistent with the fact that Ti^C is an unthermalized spin triplet while Ti^A is a thermalized one.

2. *Detailed structure analysis*

Expanded magnetic field scale spectra of Ti^A_{+1} and Ti^C_{-1} are shown in Figs. 7(a) and 7(b), respectively, exhibiting a similarity between them. The structure of Ti^A_{+1} is apparently just a broadened version of Ti^C_{-1}. These spectra were obtained with magnetic field modulation of 0.1 mT pp and $\mathbf{B} \| \hat{c}$.

The line Ti^C_{-1} was easily saturated both by excitation light and by microwave power. The best resolution was achieved with ~ 10 μW of microwaves and ~ 100 μW of excitation light. Ti^A_{+1}, on the other hand, was difficult to saturate with either microwaves or excitation light.

The structures associated with the $\Delta M = \pm 1$ transitions for both Ti^A and Ti^C are symmetric with respect to their average central magnetic field position. For example, every line in Ti^C_{-1} can be paired with a corresponding line

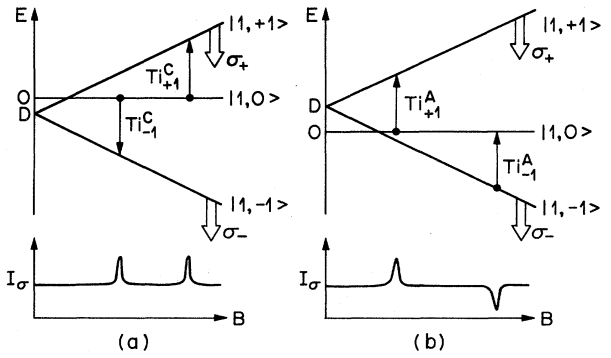

FIG. 6. Energy-level diagrams of (a) Ti^C and (b) Ti^A. The directions of the net microwave-induced transitions at resonance are indicated by the arrows. Shown also are the signs of the ODMR lines at the resonances.

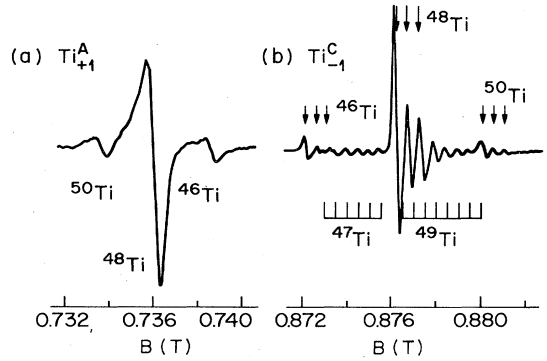

FIG. 7. Expanded magnetic field scale spectra of (a) Ti^A_{+1} and (b) Ti^C_{-1}, illustrating the isotopic structure. The insets in (b) show the hf structure arising from ^{47}Ti and ^{49}Ti.

in Ti^C_{+1}. Furthermore, the positions of the average magnetic field for each pair are identical within experimental error, indicating that the $g_{||}$ values for each pair are the same. Since the magnetic field separation between the $\Delta M=+1$ and -1 resonances is $2D/\mu_B g_{||}$ (for $|D|<h\nu$, where ν is the microwave frequency), the structure shown in the figure must arise from slightly different D values of a group of defects with identical $g_{||}$ values. This is fully consistent with the observation of *no structure* in the $\Delta M=2$ transition, Ti^C_2 (and Ti^A_2 as well), for $\theta\sim 0°$.

The relative integrated amplitudes of the lines in the structure supply a clue as to what the group of centers is. The three main groups (each group is indicated with three arrows) in Fig. 7(b) can be identified with the nonmagnetic nuclear spin $I=0$, nuclear isotopes ^{46}Ti, ^{48}Ti, and ^{50}Ti, as indicated in the figure, the integrated amplitudes matching the natural abundances 8.0%, 73.4%, and 5.3%, respectively. The other two natural isotopes, ^{47}Ti (7.8%, $I=\frac{5}{2}$) and ^{49}Ti (5.5%, $I=\frac{7}{2}$), have nonzero nuclear magnetic moments, and therefore hf splittings are expected. The hf structure of ^{47}Ti can be recognized by the six-line equal-amplitude structure centered between the ^{46}Ti and ^{48}Ti complexes. The relative integrated amplitude of the six-line structure also confirms the natural abundance of ^{47}Ti. The eight-line hf structure of ^{49}Ti is partially obscured by the structure of ^{48}Ti. The "group" of defects is therefore the same defect, but with the five different naturally occurring isotopes of Ti.

The structure indicated by the three arrows for the stronger even-nuclei isotope lines can be explained by additional isotopic shifts of the D values, due to silicon neighbors [^{28}Si (92.21%), ^{29}Si (4.70%), and ^{30}Si (3.09%)]. The ratios of the integrated amplitudes for the lines indicated with arrows match within experimental error to the predicted probabilities for various combinations of silicon isotopes in a six-equivalent-atom complex. Only the first three dominant lines are indicated with arrows in the figure. More lines with decreasing amplitudes are also predicted as the isotopic mass of the six-silicon-atom complex increases, which can be also be seen in Fig. 7(b). The asymmetric line shape of the strongest central line (^{48}Ti) could be caused by weaker isotopic shifts of silicon isotopes in more distant shells. No evidence of either isotopic shifts due to carbon atoms nor hf interaction of ^{29}Si have been detected. The entire structure of Ti^C_{-1} is therefore a convolution of naturally abundant isotope spectra of a single Ti atom and of a six-equivalent-Si-atom complex. The observed D values are listed in Table I for various combinations of isotopes.

As pointed out before, the $\Delta M=2$ transition (Ti^C_2) does not show any structure at $\theta\sim 0°$ ($\mathbf{B}||\hat{\mathbf{c}}$). However, when $\theta\sim 45°$, a three-line structure has been observed in Ti^C_2 (Ti^A_2 as well). This confirms the validity of the isotopic origin of the D-value shifts.

Similar analysis has been applied for the Ti^A spectrum, which is merely a smeared-out version of Ti^C. The asymmetric line shape of Ti^A_{+1} [see Fig. 7(a)] is evidence of unresolved isotopic structure due to silicon isotopes.

3. *Results regarding 4H and 15R polytypes*

ODMR signals observed in $4H$ and $15R$ polytype samples exhibit line shapes and spin Hamiltonian parameters which are highly similar to those seen in $6H$ samples. In the $4H$ samples, only one spin triplet, Ti^C-like, was detected. On the other hand, in the $15R$ samples, two spin-triplet defects were detected, one Ti^C-like and the other Ti^A-like. Therefore the result obtained from $6H$ samples serves as a model which provides important information

TABLE I. Spin-Hamiltonian parameters of Ti^A and Ti^C in $6H$ SiC:Ti.

	Isotopic spectrum 6-Si-atom			D (10^{-4} cm^{-1})	
Ti	28	29	30	Ti^A	Ti^C
46	6	0	0	+4936(2)	−3644(1)
	5	1	0		−3639(1)
	5	0	1		−3634(1)
	4	2	0		
48	6	0	0	+4959(2)	−3606(1)
	5	1	0		−3601(1)
	5	0	1		−3596(1)
	4	2	0		
50	6	0	0	+4979(2)	−3570(1)
	5	1	0		−3565(1)
	5	0	1		−3560(1)
	4	2	0		

	$g_{||}$	$g_\perp$	$A_{||}$ (^{47}Ti)
Ti^A	1.935(0.5)	1.945(0.5)	
Ti^C	1.957(0.5)	1.972(0.5)	$5(0.5)\times 10^{-4}$ cm^{-1}

TABLE II. Spin-Hamiltonian parameters of the Ti centers in $4H$, $6H$, and $15R$ polytypes.

		Ti^A			Ti^C		
	M_{Ti}	$4H$	$6H$	$15R$	$4H$	$6H$	$15R$
$D(10^{-4}$ cm$^{-1})$	46		+4936(2)	+4536(2)	−3724(2)	−3644(1)	−3659(2)
	48		+4959(2)	+4566(2)	−3689	−3606(1)	−3621(2)
	50		+4979(2)	+4592(2)	−3655(2)	−3570(1)	−3586(2)
$g_{\|\|}$			1.935(0.5)	1.934(0.5)	1.956(0.5)	1.957(0.5)	1.957(0.5)

for the discussion of the site dependence (see Sec. III C). The spin Hamiltonian parameters for the spin-triplet defects observed in the various polytypes are listed in Table II.

4. *Nonresonant background signal and its use*

The ODMR spectra obtained with microwave chopping [see Figs. 5(c) and 8(a)] show strong nonresonant background signals, present in the entire range of the magnetic field, as well as a sharp level-crossing signal (Ti_L^C) which appears as a "dip" of the background signal. The origin of the background signal can be interpreted as leakages from the bottleneck state to the radiative state of a spin-triplet excited state caused by a "mixture" of the states due to the perpendicular component of the microwave magnetic field (the magnetic field of the microwaves in the cavity is always perpendicular to the static magnetic field). Therefore a strong nonresonant background signal can be expected to be observed when the excited spin triplet has a very strong bottleneck feature..

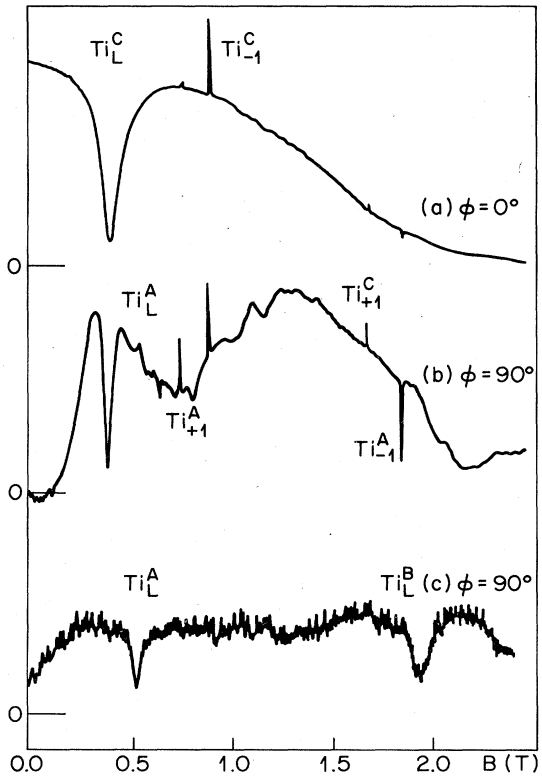

FIG. 8. Spectrum of the nonresonant background signal obtained with microwave amplitude modulation: (a) Total emission, optimized lock-in phase ($\phi=0°$) at $B=0$ T, (b) with $\phi=90°$ and with higher gain ($\times 10$), and (c) the same as (b) but only the ZPL B_0 and the 30-meV phonon replica of A (A_{30}) are detected by using a monochromator.

When the static magnetic field approaches the magnetic field position at which a level crossing can happen, the modulation in luminescence due to the microwave chopping becomes weaker, because the bottleneck feature weakens, and eventually the change in the luminescence caused by the chopping reaches zero at the level crossing. Therefore the level crossing can be observed as a "dip" of the background signal. The sharpness of the dip is a measure of alignment between the triplet defect axis and the static magnetic field direction.

The spectrum shown in Fig. 5(c) was obtained with the lock-in phase adjusted for optimum resonance signals (Ti^C), while that in Fig. 8(a) was optimized for the background signal at $B=0$ T. The nonresonant signal arises from Ti^C, as proved by a spectral dependence study (not shown in the figure). To detect the nonresonant signal arising from triplet defects other than Ti^C, the lock-in phase was shifted by 90° from the phase used for the spectrum shown in Fig. 8(a) in order to nullify the signal from Ti^C. The result is shown in Fig. 8(b), which was recorded with 10 times higher gain. It shows a rather complicated structure but it is still apparently dominated by Ti^C, as evidenced by the still strong Ti_L^C level crossing.

To eliminate any nonresonant background signal arising from the Ti^C, a monochromator was placed in front of the photodetector with wide slits (1 mm). It was tuned to ZPL, B_0. The A_{30} phonon replica (30-meV phonon replica of A) was also detected by accidental overlap. The result in Fig. 8(c) clearly shows two level-crossing "dips," one at lower magnetic field, which is Ti_L^A, as expected, and the other at higher field [1.92(2) T], which is fully consistent with the level-crossing position of Ti^B estimated from the Zeeman-splitting data of ZPL B_0 in the magneto-optical study of Dean and Hartman.[3] [Their data showed that $g_{||}\sim 1.95$, $g_{\perp}\sim 0$, and $D\sim 0.2$ meV (~ 1.6 cm^{-1}), predicting the level crossing at ~ 1.8 T for the ZPL B_0.] The D value for Ti^B therefore can be deduced from this level-crossing position with $g_{||}\sim 1.95$ to be $-1.75(2)$ cm^{-1}. The sign was obtained from the result of Dean and Hartman.[3] These "dips" become broader and eventually disappear when $\theta \gtrsim 10°$, indicating that

they are indeed level crossings. The observation of these level crossings means that both Ti^A and Ti^B have a bottleneck feature. No microwave resonances were detected, however, for Ti^B.

D. Spectral dependence study

Figure 9 shows medium-resolution spectral dependences of the luminescence, panel (a), and the ODMR lines Ti^C_{-1} [panel (b)], and Ti^A_{+1} [panel (c)] in a $6H$ sample. The luminescence spectrum shows the ZPL's (A_0, B_0, and C_0) as well as partially resolved phonon replicas [see Fig. 9(a)].

Figure 9(b) was obtained by scanning a monochromator inserted prior to the photomultiplier tube (PMT) while monitoring the ODMR line Ti^C_{-1}. It clearly shows the ZPL C_0 and its own phonon spectrum alone, resolved from the others. The spectrum shows strong 26-meV phonon replicas up to third order as well as relatively weaker but sharper 92- and 100-meV phonon replicas. The stronger 117-meV replica probably is a harmonic mixture of the 26- and 92-meV phonons. The 26- and 92-meV phonons do not match with the reported TA and LA lattice phonons,[12,13] indicating that they are characteristic "local" phonons associated with the Ti impurity. An identical result was obtained with the spectral dependence of Ti^C_L.

The spectrum shown in Fig. 9(c) was obtained by tuning the magnetic field to Ti^A_{+1} in order to get its emission spectral dependence. It shows the ZPL A_0 and its own phonon replicas alone, which are quite different from that of C: relatively weaker TA-like phonons (30 and 65 meV) and strong LA-like (90 meV) as well as optical (107 meV) phonon replicas. These phonons are similar to the lattice phonons, but with small deviations compared to the values measured by Raman scattering studies.[12]

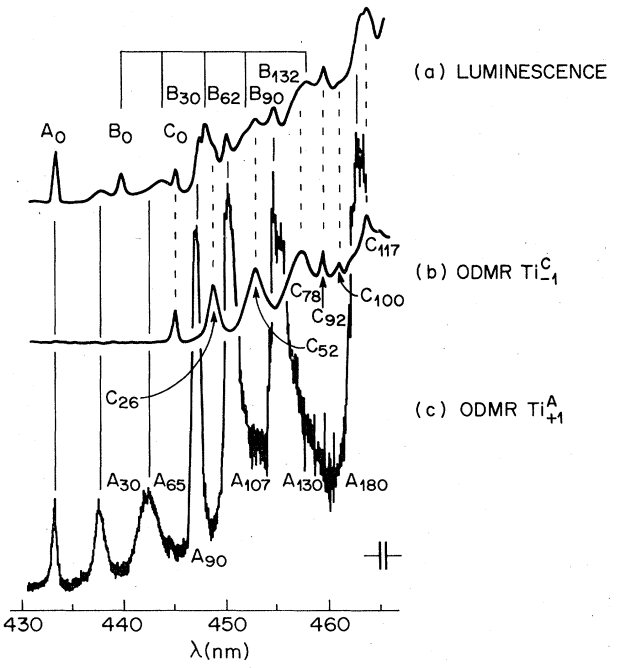

FIG. 9. Spectral dependences of (a) luminescence, (b) Ti^C_{-1}, and (c) Ti^A_{+1} ODMR lines in $6H$ SiC:Ti.

By comparing the luminescence spectrum [Fig. 9(a)] with the spectral dependences of Ti^C and Ti^A [Figs. 9(b) and 9(c), respectively], several phonon replicas, which do not belong to either A_0 and C_0, can therefore be identified as replicas of B_0 and they are indicated in the inset of Fig. 9(a). This experiment serves as a dramatic example of the power of ODMR to separately identify and resolve each of the components of partially overlapping phonon spectra. The results of Fig. 9 correct a few mistaken assignments of phonon replicas made in previous work.[14]

The emission spectral dependence of Ti^C_{-1} in the full wavelength range of the luminescence spectrum is shown in Fig. 2(c), which looks very much the same as the PL spectrum but slightly shifted toward the longer-wavelength side. A lower-resolution spectral dependence of Ti^A_{+1} (not shown in the figure) appears similar to the PL spectrum also, but shifted toward the shorter-wavelength side by A_0-C_0 difference, as expected.

Figures 2(b), 2(d), and 2(e) show the excitation spectral dependence of PL, and the ODMR signals Ti^A_{+1} and Ti^C_{-1}, respectively, revealing that the luminescence excitation is via transitions above the excitonic band gap (E_{GX}). Differences between the spectra [Figs. 2(d) and 2(e)] indicate possible contributions from direct excitation via higher excited states of the defects. All three spectra show an oscillatory feature of unknown origin.

As demonstrated above, the spectral dependence experiment not only pulls out the individual spectrum of a particular ZPL from overlapping spectra but also directly attributes the particular luminescence system to a specific ODMR signal. This is the way by which the labeling of the ODMR lines has been made.

In $4H$ samples, similar spectral dependence studies reveal that the single observed ODMR center arises from the ZPL at 444.2 nm and its phonon replicas. This ZPL had been labeled B_0 previously.[6] Since we now know that the ODMR signal is very similar to the Ti^C resonance in the $6H$ polytype, we have elected in this work, therefore, to relable the luminescence line as C_0, as shown in Fig. 1, to make the luminescence notation relate more closely to the microscopic identity of the defect. The lack of ODMR signals associated with the ZPL at 435.0 nm which had been labeled A_0 previously[15] is similar to the observation regarding B_0 in the $6H$ polytype. The failure to detect a level crossing in the circular polarization study indicates that the excited state associated with this ZPL is thermalized in the vicinity of the modulation frequency of ~ 1 kHz. It is not clear whether this ZPL is A_0-like or B_0-like, but the lack of ODMR signals seems to suggest it is B_0-like.

Similarly, in $15R$, the two spin-triplet Ti^A- and Ti^C-like spectra seen by ODMR are found to be associated with the ZPL's at 433.4 and 445.0 nm, respectively. These were previously labeled A_0 and D_0 in the old notation,[6] but we now relabel them A_0 and C_0, respectively, as in Fig. 1. The $15R$ ZPL's B_0 and C_0 in the old notation become B^1_0 and B^2_0 in our new notation.

III. DISCUSSION

A. Excited spin-triplet states

Three distinct classes of excited spin triplets (Ti^A, Ti^B, and Ti^C) have been observed in the luminescence of Ti-doped polytypes of SiC by ODMR study. The presence of ODMR lines for Ti^A and Ti^C has enabled us to accurately determine the spin Hamiltonian parameters. No ODMR lines were detected for Ti^B, except the level-crossing signal from which the zero-field splitting was estimated.

Although the ODMR spectra of Ti^A and Ti^C are remarkably similar, they have somewhat different characteristics. First of all, Ti^A is a thermalized spin triplet while Ti^C is an unthermalized one. A preliminary result of radiative-lifetime measurements[11] on the three ZPL's (A_0, B_0, and C_0) shows they all have very much the same radiative lifetime of $\sim 100\ \mu s$. The fact that the optimum modulation frequency for ODMR of Ti^C is ~ 1.25 kHz confirms that the radiative decay process is the dominant and fastest relaxation in the optical pumping cycle [$\nu_{\rm mod} \sim (2\pi\tau_{\rm rad})^{-1} \sim 1.25$ kHz]. This suggests that the spin-lattice relaxation time of the spin triplet is longer than the radiative lifetime ($T_1 \gg \tau_{\rm rad}$) and therefore Ti^C is unthermalized. Ti^A, on the other hand, was detected by ODMR signals optimized at $\nu_{\rm mod} > 10$ kHz, indicating that $T_1 < \tau_{\rm rad}$ because $\tau_{\rm rad}$ for A_0 is again $\sim 100\ \mu s$. In other words, Ti^A is a thermalized spin triplet. T_1 for Ti^A, however, could not be measured because of the limited modulation frequency of the equipment ($T_1 < 10\ \mu s$). Therefore Ti^A and Ti^C exhibit the two extreme cases of thermalization. This is why they have different signs for some of their ODMR signals.

Ti^B seems to be very much different from the other two spin triplets. The large zero-field splitting D and the unusual anisotropy of g value ($g_{\parallel} \sim 1.95$, $g_{\perp} \sim 0$) for Ti^B was pointed out by Dean and Hartman after their magneto-optical experiments.[3] The fact that $g_{\perp} \sim 0$ may explain why no ODMR has been observed for Ti^B, because the off-diagonal matrix element for magnetic dipole transitions is proportional to $g_{\perp} H_1$, where H_1 is the microwave magnetic field which is perpendicular to the static magnetic field.

B. Isotopic shift of D

The origin of the isotopic shift of the zero-field-splitting energy, D, must be a change in the electronic wave function associated with different zero-point vibrational amplitudes for each isotope. A simple Einstein model[16] for a defect predicts

$$D \sim D_0 \prod_{i=1}^{n} (1 + a_i \langle x_i^2 \rangle) \tag{2a}$$

$$\sim D_0 \left[1 + \sum_{i=1}^{n} b_i M_i^{-1/2} \right], \tag{2b}$$

where a_i and b_i are coefficients, and $\langle x_i^2 \rangle$ the mean-square vibrational amplitude of ith nucleus with mass M_i in atomic units.

From the experimental results, the above equations can be rearranged for one Ti and six Si atoms,

$$D \sim D_0 \left[1 + b_{\rm Ti} M_{\rm Ti}^{-1/2} + b_{\rm Si} \sum_{i=1}^{6} M_{\rm Si}^{-1/2} \right], \tag{3}$$

where $b_{\rm Ti}$ and $b_{\rm Si}$ are the coefficients for the Ti and Si nuclei, respectively. An accurate test of this equation is demonstrated in Fig. 10 for the observed isotopic shifts due to Ti from various polytype samples. The data points cannot be fit to a straight line when a linear isotopic mass scale is used for the horizontal axis.

The changes in the D values per unit titanium mass, $\Delta D/|D|$, are $\sim +5\times 10^{-3}$ and $\sim +2\times 10^{-3}$ for Ti^C and Ti^A, respectively. These are about 50 times larger than any other reported values for systems with comparable isotopic mass.[16,17,18] It is interesting that the shift for both Ti^A and Ti^C are *positive* even though the D values for them have opposite signs. A *positive* sign in the shift caused by the Si isotopes was also observed for all polytype samples (4H, 6H, and 15R).

The fact that the excited-state wave function is apparently so strongly dependent even upon small change in the zero-point vibrational amplitudes of the Ti and its Si neighbors reveals that the excited state is strongly vibronic in character. Additional evidence of this is the large isotopic shifts observed in the ZPL luminescence (0.13 meV per mass unit).[4] ZPL isotope shifts result from a change in vibrational frequency between ground and excited states.[19] The isotope shift for the Ti ZPL's corresponds to a reduction in the vibrational force constant by $\sim 30\%$ in the excited state, and is among the largest observed in semiconductors.[19] This brings up an important point concerning the identification of chemical elements involved in a defect by ODMR studies. The results in this work demonstrate for the first time that the isotopic structure

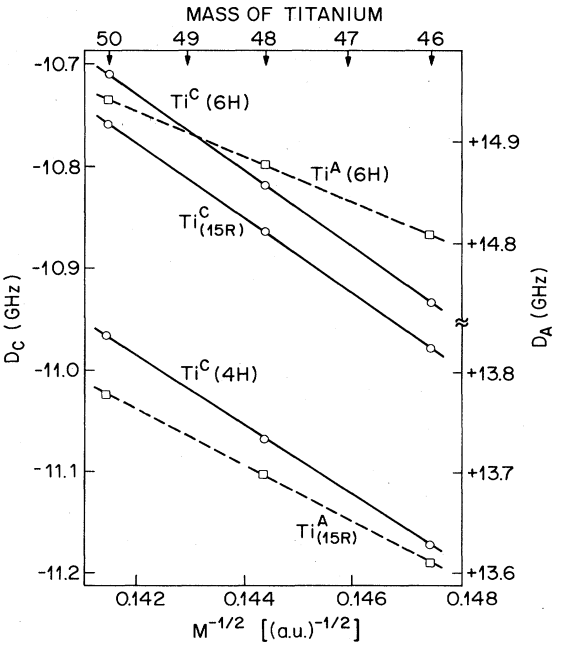

FIG. 10. Dependence of D on titanium isotopic mass M for Ti^A (squares) and Ti^C (circles) in 4H, 6H, and 15R samples.

observed in ODMR experiments can be utilized, as is hf structure, in determining the chemical identity of defect constituents. Such an isotopic spectrum may be a unique feature in systems in which isotopic shifts of ZPL's can be seen and the mechanism for the recombination process is decay of a bound exciton (in order to involve spin-triplet excited states in the optical pumping cycle).

C. Model of the Ti impurity

A single Ti atom must be involved in the defect associated with Ti^A and Ti^C because the isotropic spectrum seen in the D values for both centers can be interpreted with only *one* Ti atom. This is also consistent with the observed hf structure of ^{47}Ti in Ti^C_{-1} [see Fig. 7(b)]. The isotopic shifts observed in the ZPL's (Ref. 4—6) confirm this also for the Ti^B center.

Next is to determine the site in the crystal where the Ti impurity is located. One clue to the site is the isotopic spectrum due to six silicon atoms. There are not many sites with six equivalent silicon atoms as neighbors. Some of the interstitial sites have six silicon atoms at the next-nearest sites. However, a major difficulty for the sites' being interstitial is the fact that the observed number of ZPL's is roughly equal to the number of inequivalent *substitutional* lattice sites in the several polytypes.[6] If the Ti impurity were located at interstitial sites, it does not seem possible to match the number of inequivalent interstitial sites to the number of ZPL's unless one assumes preferential occupation for the Ti impurity at only a few of the several inequivalent interstitial sites.

On the other hand, if the Ti impurity is substitutional, then the carbon sublattice cannot be a candidate for the impurity sites, because the number of neighboring silicon atoms around the carbon site is four. The number of nearest silicon atoms for the silicon sublattice sites is 12 rather than six, requiring an assumption of a particular vibrational mode coupling to reduce the effective number of Si atoms to six. This point will be readdressed later.

The fact that the observed numbers of ZPL's in the polytypes correlate roughly with the number of inequivalent substitutional lattice sites seems to support the conclusion that the lattice site for the Ti impurity is the substitutional silicon site. This is consistent with the ligand model proposed by Patrick and Choyke[6] in which they considered $sd_{t_2}^3$ bonding between Ti and the four neighboring C atoms, leaving an empty d_e-electron orbital in the energy-band gap near the conduction-band edge. Furthermore, recent theoretical calculations for the electronic structure of substitutional and interstitial $3d$-transition-metal impurities in silicon predict an empty localized d_e orbital in the upper half of the band gap for substitutional titanium[20] but much different structure for the interstitial impurity.[21,22] This calculation therefore supports the ligand model[6] for the substitutional Ti impurity and at the same time appears to rule out the possibility that the Ti atom occupies interstitial sites.

1. Site dependence

The lattice sites labeled h and k in Fig. 1 are the hexagonal-like and cubic-like crystallographic inequivalent lattice sites, respectively, which are uniformly distributed among both Si and C sublattices. Their difference arises in their second-nearest-neighbor shell, the twelve atoms being arranged as in the cubic zinc-blende structure for the k sites and as in the wurtzite structure for the h sites. Figure 11 shows the three inequivalent lattice sites in $6H$, complete up through the third-nearest-neighbor shell. The k site in $4H$, and the k_2 and k_3 sites in $15R$, are identical in coordination to the k_2 site in $6H$ through the third-nearest-neighbor (NN) shell as shown in Fig. 11. A similar identity exists between the h sites in all polytypes as well as between the k_1 site in $6H$, the k_1 site in $15R$, and the k site in $3C$. This classification (hereafter called the "third-NN-site dependence") may be useful when the wave function of a substitutional defect is fairly localized and the crystal field of the local environment therefore plays an important role. One might expect, for instance, that a defect located at the h site would experience a stronger local axial field than ones at the k sites (see Sec. II D). This site dependence will be referred to as the "third-NN-site dependence."

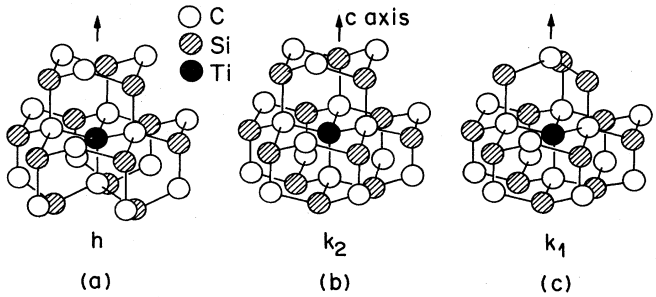

FIG. 11. Three inequivalent lattice sites: (a) h, (b) k_2, and (c) k_1 sites in $6H$ SiC, complete through the third-nearest-neighbor shell. The figure shows a Ti impurity on the silicon sublattice.

We now discuss the site dependence of the Ti impurity on the basis that the Ti atom is located on the Si sublattice and that the wave function of the bound exciton at the Ti atom is reasonably localized so that "the third-NN-site dependence" is valid.

Table III summarizes our tentative site assignments. The arguments leading to these assignments are as follows:

(i) Ti^A has been detected as a single ZPL in only $6H$ and $15R$ samples, not in $4H$ ones. This suggests the iden-

TABLE III. Summary of the tentative site assignments.

Polytypes	Ti^A	Ti^C	Ti^B
$4H$		k	h
$6H$	k_2	k_1	h
$15R$	k_3	k_1,k_2	h_1,h_2
$12R$[a]	k_2	k_1	h_1,h_2

[a]Only one Ti^C ZPL is observed in samples identified as $15R$. A $12R$ structure would correctly predict the observed number of ZPL's.

tification of the k_2 site in $6H$ and the k_3 site in $15R$ with Ti^A because they are identical through the third-NN shell and this site does not exist in $4H$ (see also Fig. 11).

(ii) Ti^C has been observed in all three polytype samples and correlated with the ZPL C_0. The similarity in the spin Hamiltonian ($g_{||} \sim g_{\perp} \sim 2.0$) between Ti^C and Ti^A suggests the assignment of the site for Ti^C to the remaining cubic sites, i.e., the k site in $4H$, k_1 site in $6H$, and k_1 and k_2 sites in $15R$ (see Sec. III D).

(iii) Ti^B has been detected as the ZPL B_0 in $6H$ SiC. The significantly different spin Hamiltonian parameters of Ti^B (large D value and the $\cos\theta$-dependent g value as observed in the magneto-optic study of Dean and Hartman[3]) suggest assignment to the remaining hexagonal h sites (an additional argument for this assignment will be given in Sec. III D).

The above assignments seem to provide a unique picture for $4H$ and $6H$ SiC. However, difficulty arises for $15R$ SiC. In $15R$ samples, the above site dependence predicts two ZPL's or two ODMR centers for Ti^C because there are two similar sites, k_1 and k_2, while the observed number of ODMR centers or ZPL's is only *one*. The fact that one ZPL is missing in $15R$ material was recognized in the early optical studies and two possibilities were suggested:[6] (1) occupancy of one of the sites is energetically unfavorable, or (2) the exciton binding energy is too weak for one of the sites. We now know that the missing ZPL is associated with a Ti^C-like site, which makes these arguments somewhat less convincing, although, of course, still possible. (The k_1 and k_2 sites are identical through third-nearest neighbors. Also the Ti^C ZPL's are the lowest-energy ones and therefore less likely candidates for weak exciton binding.)

A third possibility that has not previously been suggested is that there could be alternate stacking structures that would still provide the apparent 15-layer supercell detected by x-ray structure analysis but which would provide a closer match of inequivalent sites versus ZPL's. An interesting observation in this regard is that a $12R$ structure, also included in Table III, contains the specific combination of inequivalent lattice sites to match the optical and ODMR results. It would be interesting to perform a modern detailed atomic position x-ray structure determination either to confirm the accepted structure or to check if possibly a $12R$ or similar subunit is a major component in the $15R$ crystals. (An argument against this is the fact that a pure $12R$ polytype has not been observed, indicating that this structure may not be preferred in nature.)

There is another common polytype structure ($33R$) whose number of inequivalent sites does not match the observed ZPL's.[6] We did not have suitable samples of this polytype to study. It would be interesting to study crystals of this structure by ODMR in the future. In particular, the $33R$ polytype shows two C_0-like ZPL's and one could therefore learn what differences exist in the ODMR signals between the two Ti^C-like sites.

The site assignments given in Table III have resulted from a simple and logical deduction considering all of the optical and ODMR results and is based upon the third-nearest-neighbor model for the inequivalency of the lattice sites. However, until a satisfactory explanation is established for the missing ZPL's in the larger supercell polytypes, these assignments must still be considered tentative.

2. *Electronic structure*

The model of Patrick and Choyke[6] predicts an empty d_e level in the gap which serves as an efficient exciton trap by localizing an electron first and then binding a hole by Coulombic attraction. In other words, the electron is localized in the d_e orbital but the hole is more diffuse. This excitonic model is consistent with the observed central hf interaction for ^{47}Ti, $A \sim 5 \times 10^{-4}$ cm^{-1}, which is roughly one-half the value, $A \sim 10^{-3}$ cm^{-1}, observed for Ti^{2+} ($3d^2$) in tetrahedrally coordinated II-VI compounds[23,24] for which both spin-carrying particles are localized in the d_e orbitals.

Next let us consider the hole state. The valence-band structure of the hexagonal polytype SiC is similar to that of CdS with the Γ_9 band at the top of the valence band. This has been established both experimentally and by a theoretical band calculation for $2H$ SiC.[25] The experimental evidence includes absorption measurements in $6H$ SiC (Ref. 26) and Zeeman experiments on the sharp nitrogen D_0X line in $6H$ SiC (Ref. 3). In the absorption experiment, two absorption edges were observed separated by the spin-orbit splitting, $\lambda \sim 7$ meV, indicating that the top of the valence band involves the $\Gamma_9(P_{\pm})$ and $\Gamma_7(P_{\pm})$ manifolds split by the spin-orbit interaction. The $\Gamma_7(P_z)$ state, split off by the hexagonal crystal field, is presumed to be significantly deeper in the valence band. In the Zeeman experiment, Dean and Hartman[3] observed that the g value of the loosely bound hole (exciton binding energy is less than 33 meV) is $\sim 3.2\cos\theta$, which is characteristic of the Γ_9-like hole state.

When the hole is bound at an acceptor, two distinct parentages for the hole in the valence band have been observed: Γ_9 or $\Gamma_7(P_z)$, depending apparently on the sign of the effective crystal field experienced by the hole. For example, the relatively shallow Al acceptor ($E_A \sim E_V + 0.25$ eV in $6H$ SiC) (Ref. 27) reflects the Γ_9 valence-band states for each of the three nonequivalent substitutional polytype sites as evidenced by its anisotropic g values.[28] On the other hand, the deeper B acceptor ($E_A \sim E_V + 0.7$ eV in $6H$ SiC) (Ref. 27) has been detected as a localized spin-$\frac{1}{2}$ center with isotropic $g \sim 2.0$ for each of the sites,[29] indicating that the hole state for this localized acceptor is $\Gamma_7(P_z)$-like and the sign of the crystal field is therefore apparently *reversed* from that for the delocalized holes. These observations seem to suggest that the sign of the effective crystal field is related to the degree of localization of the hole wave function.

The magneto-optical study of $6H$ SiC:Ti done by Dean and Hartman[3] as well as this current ODMR study suggest that the hole states involved in the Ti bound-exciton states may be in a special situation in which the hole localization is intermediate, because the g values for Ti^A and Ti^C are isotropic and near 2.0, while that for Ti^B is highly anisotropic ($\cos\theta$ dependence) as deduced from the data in Ref. 3. In other words, small environmental differences (the site dependence) seem to have changed the

hole states from $\Gamma_7(P_z)$-like (Ti^A and Ti^C) to Γ_9-like (Ti^B) ones, as a result of opposite signs of their local crystal field as suggested by Dean and Hartman.[3] Consistent with this concept, the assignment in Table III of Ti^B to the hexagonal sites corresponds to the reasonable assumption that the local hexagonal field for the site is of the same sign as that determined by the crystal structure for the extended hole.

This large sensitivity of the wave function of the hole to minute environmental changes brings up an important point because the hole wave function could therefore be equally sensitive to the vibrational motion of atoms in the local environment. The observed unusually large isotopic effects in the D values reveal that the hole wave function must couple strongly to the motion of the central Ti atom. Since the symmetry of such $\Gamma_7(P_z)$ hole states is $A_1(P_z)$, it couples only to A_1-mode vibrations. Of the various symmetric mode phonons, there is an A_1-mode phonon involving the motion of the Ti atom along the hexagonal c axis of the crystal, a volume-conserving A_1-mode phonon which is a split-off phonon from the T_2 mode in T_d symmetry. Indeed, for Ti^C, the spectral dependence [see Fig. 9(b)] exhibits strong coupling to a soft TA-like phonon (26 meV, corresponding roughly to the TA-mode lattice phonon at 30 meV).[12,13] If this is correct, it may also explain why the isotopic effect due to the Si neighbors involves only six Si atoms rather than twelve atoms. Because the $\Gamma_7(P_z)$ hole is P_z-like (the z axis is along the hexagonal c axis), the coupling to the six silicon atoms above and below the plane perpendicular to the c axis and containing the Ti atom might be expected to dominate (see Fig. 11).

Evidence for strong vibronic character for the defect is also present in the large Franck-Condon shift (0.33 eV, between the zero-phonon line and the maximum of the broad phonon-assisted band, see Fig. 2) and in the unusually large isotope effect reported for the zero-phonon line,[4,19] and discussed in Sec. III B. The sign of the ZPL isotope shift reveals a softening of the lattice in the excited state which appears to confirm that it is the excited state which is the vibronic one responsible for the relaxation. Part of this relaxation energy could reflect a dynamic Jahn-Teller effect for the electron in the d_e state. The d_e state couples, however, primarily to symmetric e modes of distortion and should not therefore couple strongly to motion of the central titanium atom (rigorous in T_d symmetry). The hole part of the exciton must therefore be the source of the Ti-isotopic effects. The Franck-Condon shift energy is much greater than $\lambda \sim 7$ meV,[26] or the characteristic lattice phonons 30—120 meV,[12] or possibly even the $P_{\pm}$-P_z hexagonal crystal-field splitting which is not currently known. The contributions of this relaxation therefore clearly cannot be ignored. For instance, in the absence of the hexagonal crystal field (i.e., T_d symmetry), the electronic state occupied by the hole state would be of t_2 symmetry and energetically a symmetry-lowering lattice relaxation for the hole (Jahn-Teller effect) would always be of the sign to *raise the nondegenerate P_z state* (the energy of the P_z hole state would be lowered). This is of opposite sign to the built-in hexagonal field. As the hole state localizes, the Jahn-Teller effect becomes more important (because the competing elastic energy stored in the lattice is proportional to the volume of the hole orbit). Conversely, the Jahn-Teller effect serves to localize the hole. This cumulative effect therefore, and its competition in sign to the built-in hexagonal crystal field, could be an important contributing factor in the apparent high sensibility of the site dependence to the character of the hole state. At the same time, it is important to keep in mind also that both the $P_{\pm}$ hole states (and the d_e-electron states) remain degenerate in the hexagonal field and *dynamic* Jahn-Teller effects may also be important. In addition to contributing to relaxation energies and localization, they also serve to reduce orbital contributions to g values, spin-orbit interactions, etc., which can have profound effects on the spin Hamiltonian.[30] Evidence of this is found in the g values for the Ti^B center. The $\cos\theta$ anisotropy reveals the $\Gamma_9(P_{\pm})$ origin for the hole, but the $g_{\parallel} \sim 2$ reveals the quenching of the orbital contribution.[28]

There are still other effects that can come into play as the hole state localizes. As the hole localizes it will take on more of the d_{t_2} localized character of the Ti ion. The signs of the crystal-field coupling parameters and orbital matrix elements for a d_{t_2} state are reversed from extended t_2 p-like orbitals,[31–33] again giving a mechanism for crystal-field sign reversal.

On the basis of our present results, we cannot distinguish the relative contribution of these effects for the titanium centers. However, the fact that they all depend critically on the degree of hole localization, and the evidence for substantial lattice relaxations and vibronic effects, suggest that the Jahn-Teller hole coupling may play an important role.

This question of the parentage of bound hole states is also one of current interest and speculation for defect systems in other semiconductors.[34,35] The fact that makes the Ti centers in SiC so remarkable and unique is the apparent reversal of the local crystal field between sites so closely identical. The effects that we have discussed here, not previously considered, may be relevant in these other systems as well.

IV. CONCLUSIONS

Three distinct excited spin triplets, Ti^A, Ti^B, and Ti^C, have been observed in polytypes ($4H$, $6H$, and $15R$) of SiC single crystals containing Ti by using ODMR. The studies of the spectral dependence for the ODMR lines have provided a direct correlation of Ti^A and Ti^C with the ZPL's A_0 and C_0, respectively. Characteristic phonons associated with Ti^A and Ti^C have also been resolved from the overlapping luminescence spectrum and those for Ti^B, in turn, indirectly deduced.

The analysis of the resolved structure in the ODMR lines associated with Ti^A and Ti^C has revealed that the structure arises from an unusually strong isotopic shift in the zero-field splitting energy, D, of the spin triplets. The isotopic structure has been interpreted as a convolution of two independent isotope spectra: the naturally abundant five Ti isotopes and the three Si isotopes in a neighboring six-silicon-atom complex.

The isotopic shift due to Ti isotopes identifies the defect as an isolated Ti impurity, and that due to the six silicon ligands suggests that this impurity is located on the silicon sublattice. With the ODMR results obtained for $4H$ and $15R$ samples, tentative inequivalent lattice site assignments have been made for the A, B, and C systems. This site dependence reveals a remarkable sensitivity of the defect to small environmental changes. Differences only in the second-nearest-neighbor shell strongly affect the electronic structure of the defect. This sensitivity has been discussed in terms of a possible instability regarding the localization of the hole in the bound-exciton state of the Ti impurity as Jahn-Teller coupling of the hole competes with the internal hexagonal crystal field. (In this model the electron is tightly bound in the d_e shell of the Ti atom.) The observation of the large isotopic shift was also cited as evidence for this vibronic sensitivity, by which the wave function of the bound exciton could easily be modulated when a particular mode of phonon is coupled.

V. ACKNOWLEDGMENTS

Helpful discussions with F. S. Ham are gratefully acknowledged. One of us (K.M.L.) would like to thank the Sherman Fairchild Foundation for financial support. Continued collaboration between Lehigh University and the Laboratoire de Spectrometrie Physique has been made possible by a NATO grant. The research was supported by NSF Grants Nos. DMR 77-11-309 and DMR 80-21-065.

*Present address: AT&T Bell Laboratories, 600 Mountain Avenue, Murray Hill, NJ 07974.

†Permanent address: Laboratoire de Spectrometrie Physique, Boite Postale 53, 38041 Grenoble, France.

[1]For a recent review on the properties of SiC, see Y. M. Tairov and Y. A. Vodakov, *Electroluminescence,* Vol. 17 of *Topics in Applied Physics,* edited by J. I. Pankove (Springer-Verlag, Berlin, 1977), p. 31.

[2]D. R. Hamilton, W. J. Choyke, and L. Patrick, Phys. Rev. **131**, 127 (1963).

[3]P. J. Dean and R. L. Hartman, Phys. Rev. B **5**, 4911 (1972).

[4]W. J. Choyke and L. Patrick, in *Silicon Carbide 1973* (University of South Carolina Press, Columbia, 1974), p. 261.

[5]A. W. C. Van Kemenade and S. H. Hagen, Solid State Commun. **14**, 1331 (1974).

[6]L. Patrick and W. J. Choyke, Phys. Rev. B **10**, 5091 (1974).

[7]K. M. Lee, Le Si Dang, G. D. Watkins, and W. J. Choyke, Solid State Commun. **37**, 551 (1981).

[8]M. Channel, R. Chicault, and Y. Merle d'Aubigné, J. Phys. B **9**, 87 (1976).

[9]K. M. Lee, Rev. Sci. Instrum. **53**, 702 (1982).

[10]K. M. Lee and G. D. Watkins, Phys. Rev. B **26**, 26 (1982).

[11]E. Lightowlers (private communication).

[12]D. W. Feldman, J. H. Parker, Jr., W. J. Choyke, and L. Patrick, Phys. Rev. **173**, 787 (1969).

[13]L. Patrick, Mater. Res. Bull. **4**, 5129 (1969).

[14]W. J. Choyke and L. Patrick, Phys. Rev. **127**, 1868 (1968).

[15]D. G. Thomas, J. J. Hopfield, and W. M. Augustyniak, Phys. Rev. **140**, A202 (1965).

[16]G. D. Watkins, Solid State Commun. **17**, 1205 (1975).

[17]S. A. Marshall, J. A. Hodges, and R. A. Serway, Phys. Rev. **133**, A1427 (1964).

[18]S. A. Marshall, J. A. Hodges, and R. A. Serway, Phys. Rev. **136**, A1924 (1964).

[19]V. Heine and C. H. Henry, Phys. Rev. B **11**, 3795 (1975).

[20]A. Zunger and V. Lindefelt, Phys. Rev. B **27**, 1191 (1983).

[21]G. G. DeLeo, G. D. Watkins, and W. B. Fowler, Phys. Rev. B **23**, 1851 (1981).

[22]A. Zunger and V. Lindefelt, Phys. Rev. B **26**, 5989 (1982).

[23]J. Schneider and A. Rauber, Phys. Lett. **21**, 380 (1966).

[24]J. J. Davies, J. E. Nicholls, and D. Verity, J. Phys. C **13**, 1291 (1980).

[25]F. Herman, J. P. Van Dyke, and R. L. Kortum, Mater. Res. Bull. **4**, 5167 (1969).

[26]R. G. Humphreys, D. Bimberg, and W. J. Choyke, in Proceedings of the 15th International Conference on the Physics of Semiconductors, Kyoto 1980 [J. Phys. Soc. Jpn. Suppl. **49**, 619 (1980)].

[27]M. Ikeda, H. Matsunami, and T. Tanaka, Phys. Rev. B **22**, 2842 (1980).

[28]Le Si Dang, K. M. Lee, G. D. Watkins, and W. J. Choyke, Phys. Rev. Lett. **45**, 390 (1980).

[29]H. H. Woodbury and G. W. Ludwig, Phys. Rev. **124**, 1083 (1961).

[30]F. S. Ham, in *Electron Paramagnetic Resonance,* edited by S. Geschwind (Plenum, New York, 1972), Chap. 1.

[31]J. S. Griffith, *The Theory of Transition-Metal Ions* (Cambridge University Press, London, 1961), pp. 283ff.

[32]F. S. Ham and G. W. Ludwig, in *Proceedings of the First International Conference on Paramagnetic Resonance,* edited by W. Low (Academic, New York, 1963), Vol. I, p. 130.

[33]References 31 and 32 do not discuss the change of sign for the axial crystal field. This results from the different spatial distribution for the P_z ($\sim z$) versus the t_{2z} ($\sim xy$) states.

[34]H. P. Gislason, B. Monemar, P. J. Dean, and D. C. Herbert, Physica **117&118B**, 269 (1983).

[35]G. Davies (unpublished).